Supplementary Information

Cathodic NH_4^+ Leaching of Nitrogen Impurities in CoMo Thin-film Electrodes in Aqueous Acidic Solution

Weilai Yu[a] , Pakpoom Buabthong[b], Carlos G. Read[a], Nathan F. Dalleska[c], Nathan S. Lewis[a], Hans-Joachim Lewerenz[b], Harry B. Gray[a*] and Katharina Brinkert[a,d*]

a. Division of Chemistry and Chemical Engineering, California Institute of Technology, 1200 E California Blvd., Pasadena, CA 91125, USA.

b. Division of Engineering and Applied Science, California Institute of Technology, 1200 E California Blvd., Pasadena, CA 91125, USA.

c. Environmental Analysis Center, Division of Geology and Planetary Science, California Institute of Technology, 1200 E California Blvd., Pasadena, CA 91125, USA.

d. Department of Chemistry, University of Warwick, Gibbet Hill Road, Coventry, CV4 7AL, UK.

Email: hbgray@caltech.edu; katharina.brinkert@warwick.ac.uk

Experimental

Electrode preparations

n-type Si wafers (111, As-doped, resistivity < 0.005 Ω · cm, 3" diameter) were obtained from Addison Inc. To remove the surface oxide, the Si substrate was etched for 1 min in a buffered HF etchant (6:1 volume ratio of 40% NH_4F(aq) to 49% HF(aq)). All solutions were made from ultrapure water and analytical grade chemicals having an organic impurity level < 50 ppb.

Sputtering using a high-vacuum magnetron-sputtering system (AJA International Inc.) was performed at a constant Ar flow of 20 sccm and a working pressure of 5 mTorr. The Ti adhesion layer was directly sputtered onto the freshly etched n^+-Si wafer substrate using direct-current (DC) mode at 60 W for 35 min. The substrates were maintained at room temperature during the sputtering process. The CoMo thin-film was then co-sputtered in radio frequency (RF) mode by simultaneously keeping the Co target at 150 W and the Mo target at 100 W, while under a constant Ar flow of 20 sccm for 1 h. FeMo and NiMo were deposited using an analogous procedure in which the sputtering power for Fe and Mo targets was the same as that for Co. Sputtering of the single-element Co and Mo thin films was performed with the target maintained for 1 h at 150 W and 100 W, respectively.

The wafer was cut into ~1.2 cm^2 pieces and ohmic contacts to the electrodes were formed by rubbing an In-Ga eutectic onto the unpolished back sides of the Si samples. Conductive Ag paste was applied to attach a Sn-plated Cu wire to the ohmic contact. The wire was threaded into a glass tube and the sample was encapsulated and sealed to the glass tube using black, chemically resistant epoxy (Loctite 9460).

Electrochemical nitrogen reduction in aqueous and non-aqueous electrolytes

Electrochemical experiments were performed using BioLogic SP-200 potentiostats (Biologic, Grenoble, France) controlled by standard EC-Lab software. The experiments were performed in a standard three-electrode potentiostatic arrangement in a sealable electrochemical cell. A Pt wire (ALS Co., Ltd) was used as the counter electrode and Ag/AgCl (3 M KCl, WPI Europe, DRIREF-5) was used as the reference

electrode. No Pt deposits were observed by XPS on the catalyst (working electrode) surface after electrochemical testing. All potentials are referenced herein, unless otherwise specified, relative to the potential of the reversible hydrogen electrode (RHE). The electrolyte was 20 mL of 50 mM aqueous or ethanolic H_2SO_4. Prior to the measurements, the electrolyte was purged for 10 min with Ar (5.0 purity, flow rate 165 mL min^{-1}) under gentle stirring to remove O_2(g) from the electrolyte. To saturate the electrolyte with N_2 prior to electrochemical measurements, the electrolyte was purged for 15 min with 99.999% pure N_2 (flow rate 95 mL min^{-1}). Before entering the electrochemical (EC) cell, N_2 and Ar were directed through a gas bubbler that contained 50 mM H_2SO_4(aq).

Cyclic voltammetric and chronoamperometric measurements were performed on electrodes under a constant N_2 flow (95 mL min^{-1}). For isotope labelling experiments, the electrolyte was purged with $^{15}N_2$ instead of $^{14}N_2$ (Sigma-Aldrich, product no. 364584-5L) for 10 min prior to electrochemical tests. Before entering the electrochemical cell, the $^{15}N_2$ gas was directed through an acid-trap that contained 5 mL of 50 mM H_2SO_4(aq). Electrochemical tests were performed under a continuous $^{15}N_2$ purge. Three independent tests were carried out for each condition using freshly prepared electrodes to produce the error bars in Figure 1 in the main text. After sampling electrolyte in the cell at different stages of the experiment, the same amount of fresh electrolyte was added back into the cell to keep the total volume of electrolyte constant.

Determination of ammonium, nitrate and nitrite concentration by IC

Ammonium concentrations were determined using a Dionex (Sunnyvale CA, now Thermo) ICS 2000. The sample solutions were diluted to a certain ratio and loaded into a 5 μL sample loop by an AS40 autosampler. The sample was then injected onto a CS16 separator column (2 x 250 mm) that was protected by a CG16 guard column (2 x 50 mm). Isocratic methanesulfonic acid eluent at 20 mM and pumped at 0.25 mL min^{-1} was produced using an eluent generator cartridge based on methylsulfonic acid. Analytes were detected by suppressed conductivity detection using a Dionex CERS-500 2 mm suppressor operated in eluent recycle mode with an applied current of 15 mA. Concentrations were calculated using

Chromeleon 6.8 software.

The concentration of hydrazine was determined below the detection limit in the electrolyte by the Watt and Chrisp method.[1]

$^{14}NH_4^+/^{15}NH_4^+$ derivatization with dansyl chloride and analysis by UPLC-MS

Detection of $^{14}NH_4^+$ and $^{15}NH_4^+$ as dansyl chloride derivation products was performed on an Acquity I-Class UPLC coupled to a Xevo G2-S Quadrupole Time-of-Flight (QTof) mass spectrometer (both from Waters Corporation).[2] Dansyl chloride derivatization was performed by preparing solution mixtures in the following order in 2 mL glass vials: 0.4 mL of ~ 290 μM dansyl chloride (Sigma Aldrich, ≥ 99.0%, for HPLC) was dissolved in acetonitrile (UPLC grade). Subsequently, 0.3 mL of sodium carbonate stock solution (2 g/100 mL) and 0.4 mL of collected electrolyte in 50 mM H_2SO_4(aq) were added to the vials. The vials were vortexed for 10 s before loading onto the autosampler plate for analysis. To achieve effective derivatization without heating the samples, the pH of the sample solution was adjusted between 9 and 10 using pH paper. The derivatization products (dansyl-ammonia adducts) in the sample solution were separated by reverse phase chromatography with a binary water/acetonitrile solvent and a steady gradient. The concentration was quantitatively determined by calculating the peak area at specific mass positions (m/z = 251.0854 a.u. for ^{14}N and z = 252.0825 a.u. for ^{15}N, resp.). Data analyses were performed using the Quanlynx software and each collected sample was measured three times for accurate concentration determination.

Materials characterization

Atomic-force microscopy (AFM) images were obtained on a Bruker Dimension Icon or a Mutimode 8 using Bruker ScanAsyst-Air probes (silicon tip, silicon nitride cantilever, spring constant: 0.4 N/m, frequency: 50-90 kHz), operating in the ScanAsyst mode. The scan sizes were 1 μm x 1 μm. Images were analyzed using the Nanoscope Analysis software (version 1.9).

For transmission-electron microscopy (TEM), samples of the films were prepared using a focused Ga-ion beam (FIB) on a FEI Nova-600 Nanolab FIB/FESEM. Pt and C protection layers were deposited before exposure of the sample to the FIB. High-resolution TEM (HRTEM) images were obtained using a Tecnai Polara (F30) TEM at an accelerating voltage of 300 keV.

Scanning-electron micrographs (SEMs) were obtained with a FEI Nova NanoSEM 450, at an accelerating voltage of 5.00 kV with a working distance of 5 mm and an in-lens secondary electron detector.

X-ray photoelectron spectroscopy

X-ray photoelectron spectroscopy (XPS) was performed using a Kratos Axis Ultra system with a base pressure of 1 x 10^{-9} torr in the analysis chamber. A monochromatic Al Kα source was used to irradiate the sample with X-rays (1486.7eV) at 450 W. A hemispherical analyzer oriented for detection along the sample surface normal was used for maximum depth sensitivity. High-resolution spectra were acquired at a resolution of 25 meV with a pass energy of 10 eV. The data were analyzed using CasaXPS computer software. First, the spectra were calibrated by referencing the C 1s peak position to 284.8 eV. Co 2p, Mo 3d, N 1s peaks were then fitted to multiple subspecies each having Gaussian-Lorentz peak shapes.

Peak assignments were based on previous reports.[3–5] The transmission function (T) of the analyzer was recorded automatically during the time of measurement. The relative sensitivity factors (RSF) of each element were provided by the instrument manufacturer, and the inelastic mean free path (IMFP) of photoelectrons at different kinetic energies was calculated using Quases imfptpp2m computer software.

Surface compositions of each element were calculated by comparing the area of the peaks for each element normalized by (RSF*T*IMFP).

XPS data were obtained ex-situ i.e., after a short sample transfer through air, which could potentially confound linking the surface composition and oxidation states found in UHV to the ones present during electrocatalysis.

Determination of NO/NO_2(g) concentration in Ar and $^{14}N_2$ gases

Approximately 15 L of a gas sample was collected from an Ar/N_2 cylinder (ultra-high purity, Airgas) and stored in a Teflon bag before further analysis. A chemiluminescence $NO/NO_2/NO_X$ Analyzer (Teledyne Model T200) was used to measure the NO and NO_2 concentrations in the gas sample at a 200 cm^3 min^{-1} flow rate. The measurement had an uncertainty of 0.5 ppb. The concentration was recorded after ~ 15 min of equilibration between the gas, sampling line, and chemiluminescence chamber inside the instrument.

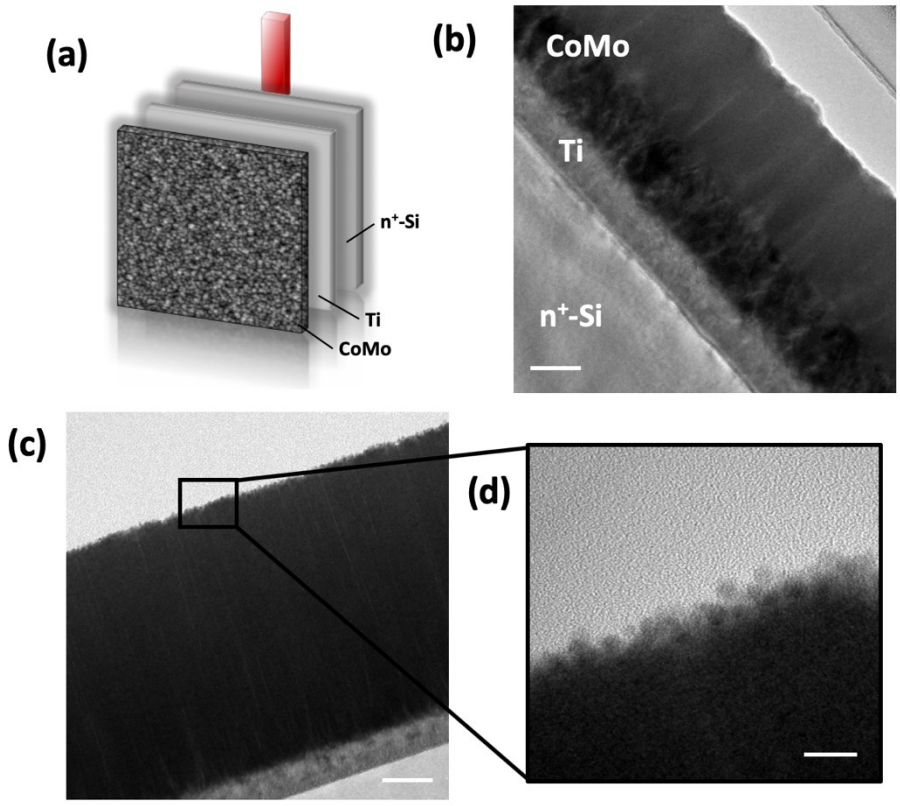

Figure S1. (a) Scheme of the n^+-Si-Ti-CoMo electrode composition; **(b)** cross-section TEM image of the n^+-Si-Ti-CoMo electrode structure as-prepared; **(c)** HR-TEM image of the CoMo surface after 12 h testing at -0.54 V *vs.* RHE in 50 mM $H_2SO_{4(aq)}$ and **(d)** magnification of **(c)**. The scale bars are: **(b)** 100 nm; **(c)** 100 nm and **(d)** 10 nm.

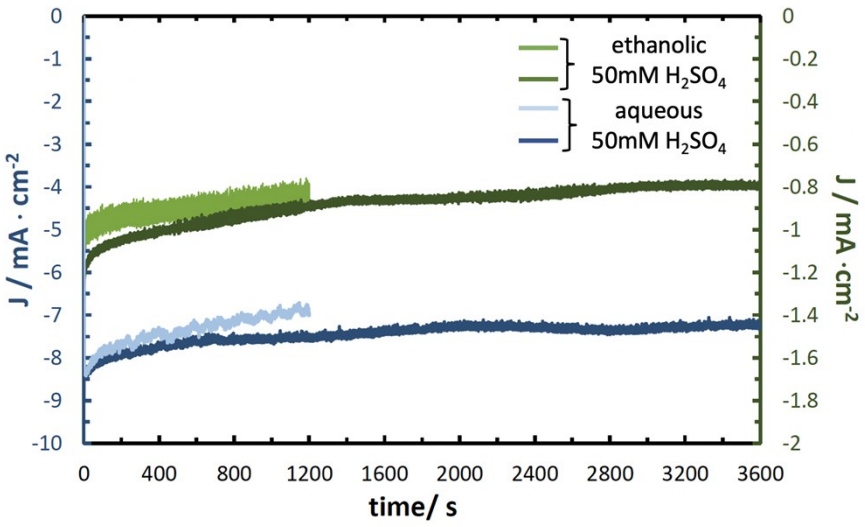

Figure S2. Chronoamperometric (CA) measurements of an n^+-Si/Ti/CoMo electrode in aqueous 50 mM H_2SO_4 (blue) and 50 mM H_2SO_4 in ethanol (green).

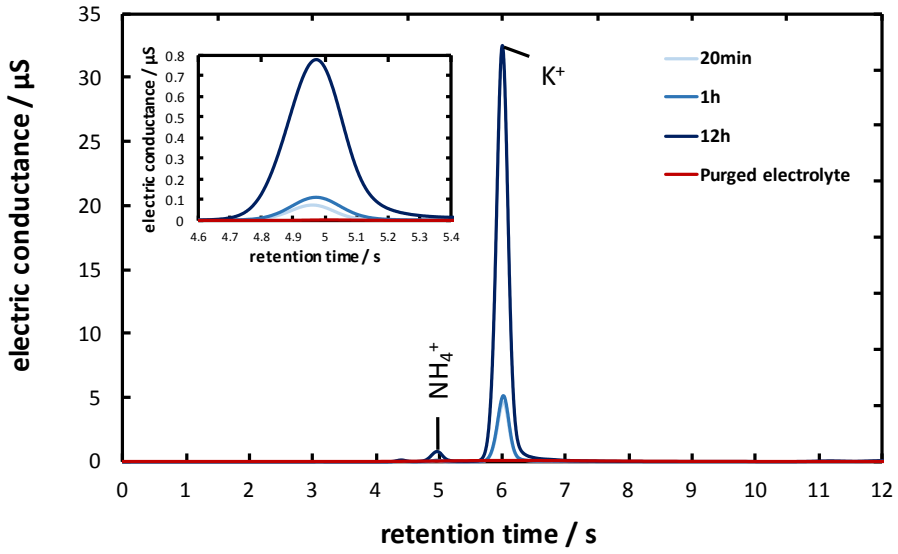

Figure S3. Ion chromatogram of the electrolyte (red) and after 20 min (light blue), 1 h (cyan) and 12 h (dark blue) electrocatalysis of n^+-Si/Ti/CoMo electrode system in aqueous 50 mM H_2SO_4 at -0.54V *vs.* RHE. The inset shows the NH_4^+ chromatogram at a higher resolution. K^+ was introduced through the junction of Ag/AgCl (3 M KCl) reference electrode.

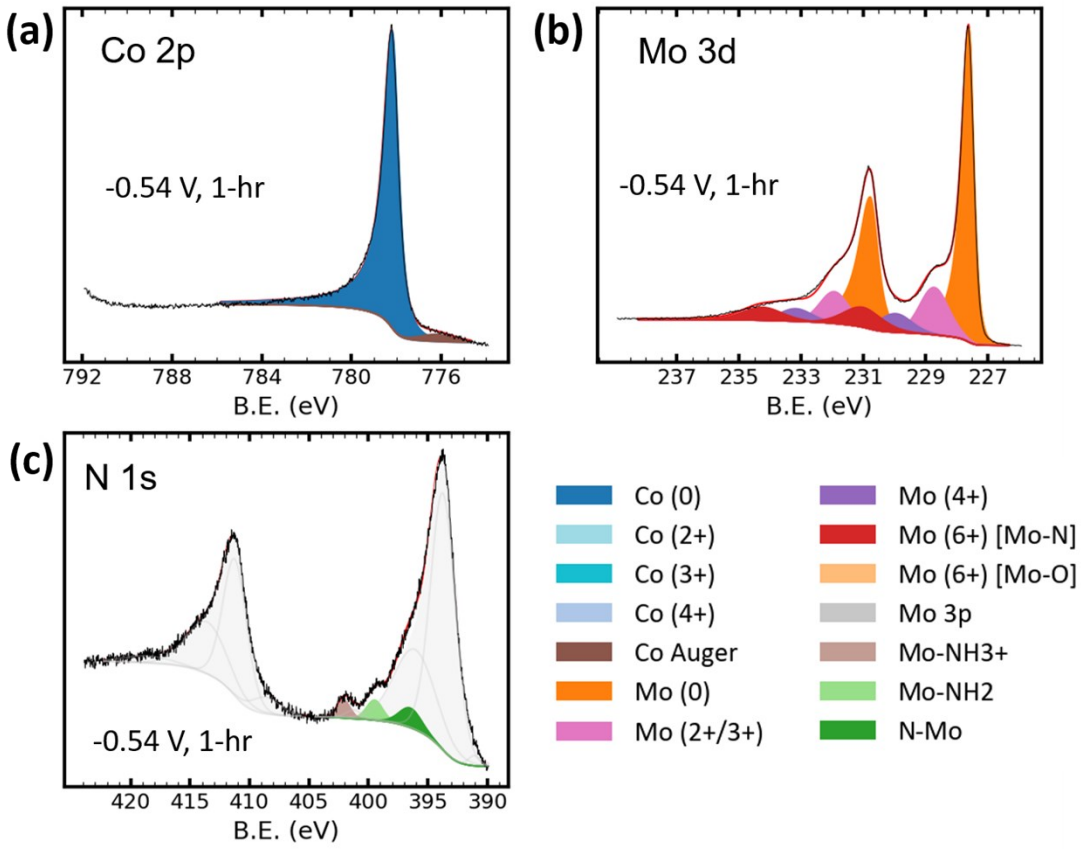

Figure S4. X-ray photoelectron spectra of the n^+-Si/Ti/CoMo surface after 1 h of electrocatalysis in aqueous 50 mM H_2SO_4 electrolyte at -0.54V *vs* RHE. **(a)** Co 2p core levels; **(b)** Mo 3d core levels and **(c)** N 1s core levels. Color coding is given in the legend; B.E is the binding energy.

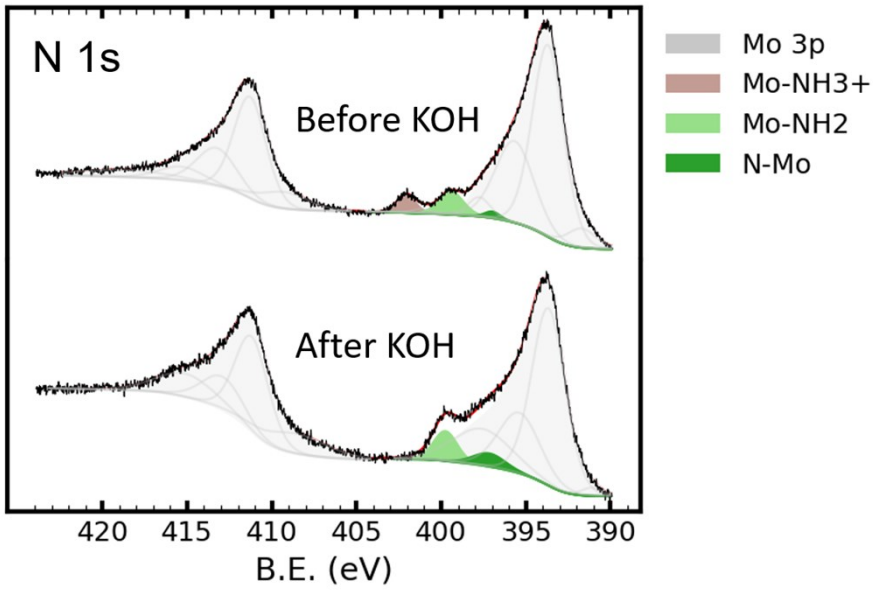

Figure S5. N 1s core level X-ray photoelectron spectra of the CoMo surface after being held for 20 min at -0.54V *vs.* RHE in an aqueous 50 mM H_2SO_4 electrolyte (top) and after incubation of the electrode afterwards for 10 min in 10 mM KOH (bottom). Color coding is given in the legend; B.E is the binding energy.

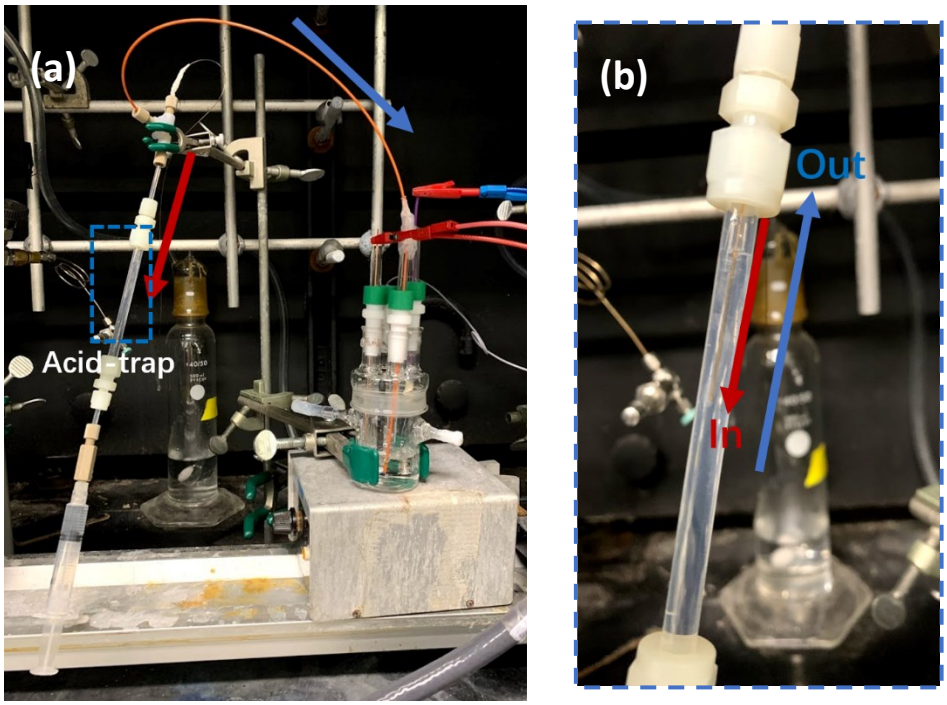

Figure S6. (a) Photograph of our electrochemical experimental setup for purging with $^{15}N_2$ gas in the presence of an acid-trap **(b)**. The $^{15}N_2$ gas was directed through a plastic tube containing a solution of 50 mM H_2SO_4(aq) before going into the EC cell.

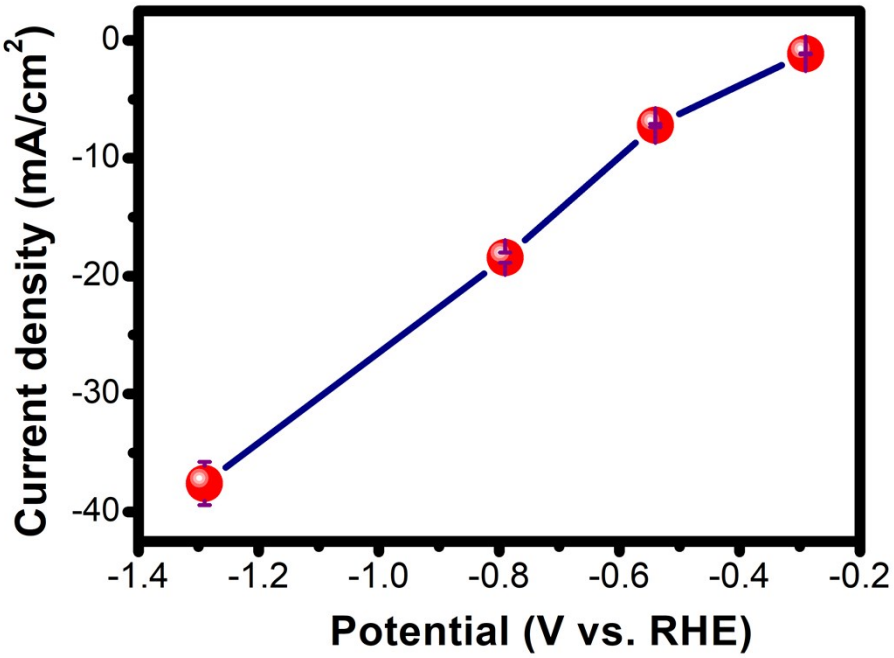

Figure S7. Comparison of averaged current density of CoMo electrodes at different potentials under constant $^{15}N_2$ purging.

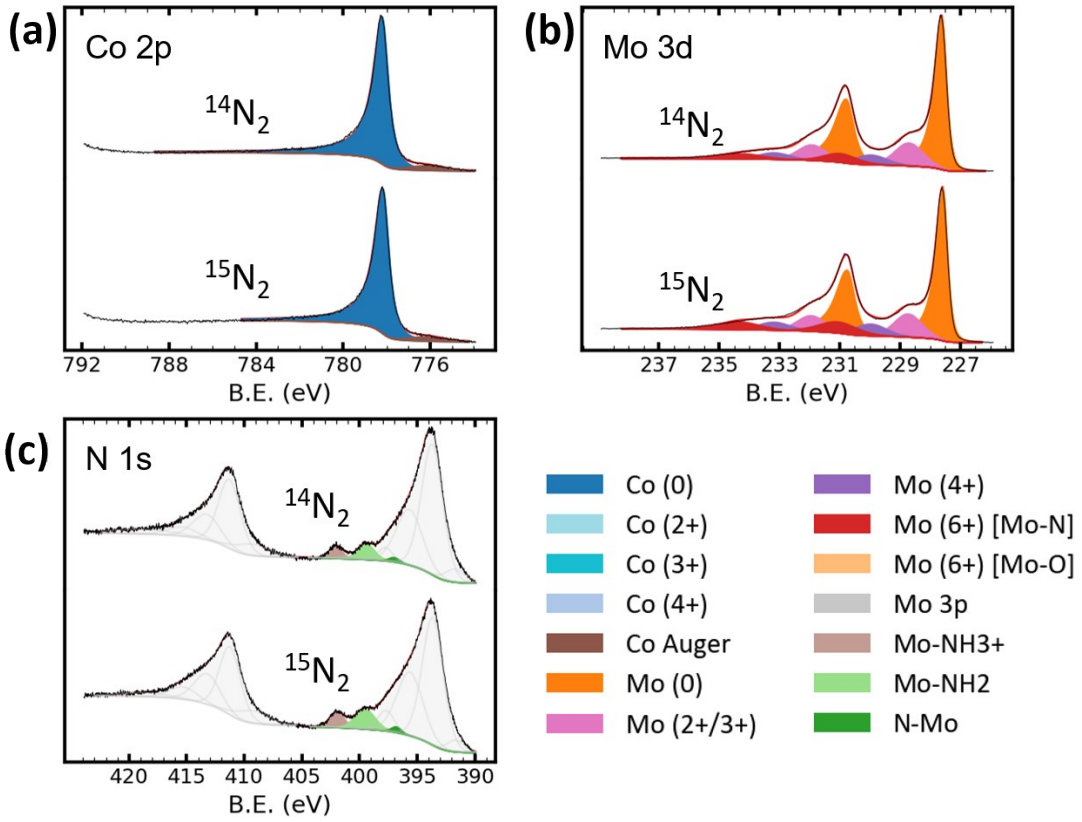

Figure S8. X-ray photoelectron spectra of the n^+-Si/Ti/CoMo surface after 20 min of electrocatalysis in aqueous 50 mM H_2SO_4 electrolyte at -0.54 V *vs.* RHE under $^{14}N_2$ purging (top) and $^{15}N_2$ purging (bottom). **(a)** Co 2p core levels; **(b)** Mo 3d core levels and **(c)** N 1s core levels. Color coding is given in the legend; B.E. is the binding energy.

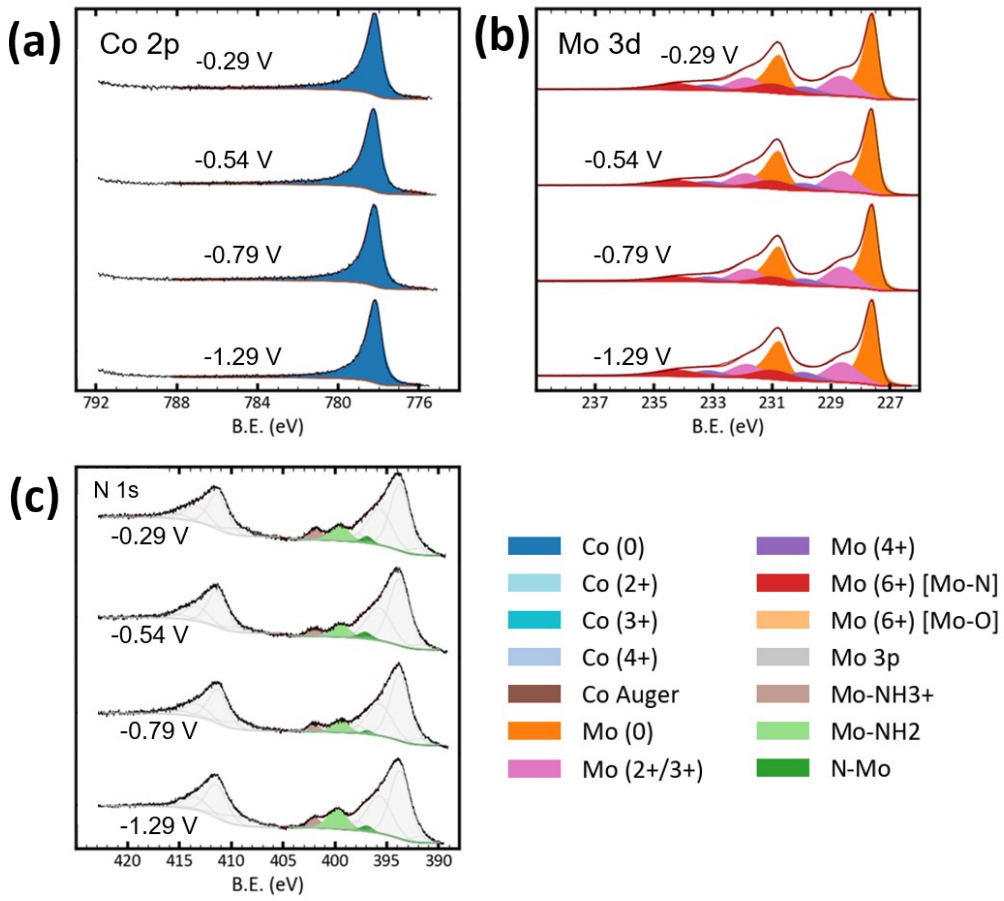

Figure S9. X-ray photoelectron spectra of the n^+-Si/Ti/CoMo surface after 20 min of electrocatalysis in aqueous 50 mM H_2SO_4 electrolyte at four different potentials vs. RHE. **(a)** Co 2p core levels; **(b)** Mo 3d core levels and **(c)** N 1s core levels. Color coding is given in the legend; B.E. is the binding energy.

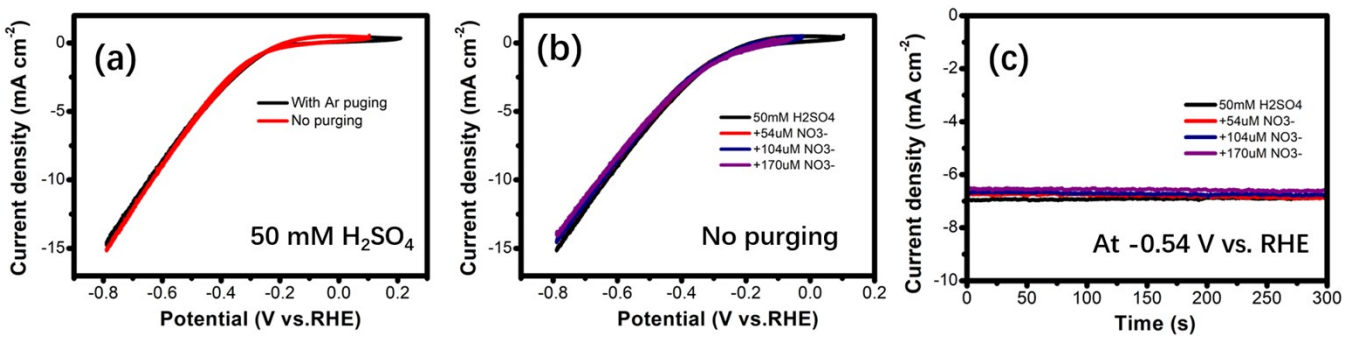

Figure S10. (a) Comparison of cyclic voltammograms (CVs) obtained at the CoMo electrode tested in 50 mM H_2SO_4(aq) with Ar(g) purging and without purging. (b) Comparison of CVs (CoMo electrode) tested in 50 mM H_2SO_4(aq) without purging in the presence of different concentrations (0, 54, 104, 170 μM) of nitrate ions (scan rate: 20 mV s^{-1}). (c) Comparison of chronoamperometry (CA) at the CoMo electrode held at -0.54 V vs. RHE in 50 mM H_2SO_4(aq) without purging in the presence of different concentrations (0, 54, 104, 170 μM) of nitrate ions.

Table S1. Measured NH_4^+ concentrations by IC obtained from various control experiments. The NH_4^+-production yield in Table 1 (main text) is corrected against these background NH_4^+ values under corresponding conditions. The total volume of electrolyte is 20 mL.

Control Experiment	t [min]	c(NH_4^+) [µM]	Total amount [nmol]
50 mM H_2SO_4		1.1	22
CoMo at E_{oc}	20	1.4	28
CoMo at E_{oc}	60	2.6	52
CoMo at E_{oc}	720	2.8	56
NiMo at E_{oc}	20	1.4	28
FeMo at E_{oc}	20	1.7	34
Co at E_{oc}	20	1.0	20
Mo at E_{oc}	20	2.5	50
CoMo at E_{oc} in 50 mM HCl	20	1.9	38
CoMo at E_{oc} in 50 mM $HClO_4$	20	2.3	46
50 mM H_2SO_4, Ar/N_2 Purge	20	0.8	16
50 mM H_2SO_4, Ar/N_2 Purge	60	0.7	14
50 mM H_2SO_4/Ethanol, Ar/N_2 Purge	20	2.0	40
Pt wire in 50 mM H_2SO_4	20	0.9	18
Pt wire in 50 mM H_2SO_4/Ethanol	20	2.5	50

Table S2. Summary of the peak positions in the XPS analysis.[3–5]

Species	Binding energy [eV]
Co^{0}	778.2
Co^{2+}	781
Co^{3+}	782.7
Co-OH	786.5
$Mo^{2+/3+}$	228.7-228.8
$Mo^{3+/4+}$	230.2
Mo^{6+}	231.2-232.5
$Mo^{d+}(2 < d < 4)$	229.97
Mo-N	397.2
$NH_{ad}/NH_{2,ad}$	399.4
$NH3_{,ad}^{+}$	402.1

Table S3. Comparison of electrode area-normalized increases in $^{14}NH_4^+$ ion concentration determined by the dansyl chloride derivatization/UPLC-MS method, after electrochemical tests using CoMo electrodes under various potential and gas-purging ($^{15}N_2$/Ar) conditions. The values correspond to the data points shown in Figure 5 in main text.

Entry	E [V *vs.* RHE]	Purged gas[a]	Increased c($^{14}NH_4^+$) [μM · cm^{-2}]
1	-0.29	$^{15}N_2$	3.2±0.1
2	-0.54	$^{15}N_2$	3.9±0.4
3	-0.54	$^{15}N_2$	6.9±0.2
4	-0.79	$^{15}N_2$	7.9±0.3
5	-1.29	$^{15}N_2$	17.9±0.7
6	-0.29	Ar	3.2±0.2
7	-0.54	Ar	3.7±0.03
8	-0.54	Ar	6.3±0.3
9	-0.54	Ar	7.9±0.2
10	-0.79	Ar	9.6±0.5
11	-1.29	Ar	6.8±0.4

[a]All purged gases were first passed through a gas bubbler of 50 mM H_2SO_4(aq).

Table S4. Comparison of nitrate (NO_3^-) concentration measured by IC in the electrolyte samples collected at different experiment stages for four independent experiments.

Entry[a]	Gas	c(NO_3^-) before purge [μM]	c(NO_3^-) after purge [μM]	c(NO_3^-) after EC[b] [μM]	$^{14}NH_4^+$ yield [μM]
1	^{15}N	14.2	12.6	17.1	9.8
2	^{15}N	10.9	5.3	18.8	3.2
3	Ar	21.5	10.7	18.1	6.3
4	Ar	18.9	4.9	16.4	7

[a]All electrochemical experiments were performed at -0.54 V *vs.* RHE. The electrolyte volume was 20 mL. The concentrations of nitrite ions were below the detection limit for all electrolyte samples. [b]EC represents electrochemical experiments

The 50 mM sulfuric acid stock solution had low concentrations (1.8 μM) of nitrate ions, which increased to >10 μM after transferring to the electrochemical cell possibly due to the additional contaminants in the cell. After 10-min of purging of both $^{15}N_2$ and Ar gas, the nitrate concentrations consistently decreased in four independent tests. This behavior indicated that continuous purging of $^{15}N_2$/Ar might have removed volatile HNO_3 species from the solution, instead of introducing additional NO_3^- into the electrolyte. In comparison, only a slight increase (6.9 μM) in the concentration of nitrate ions was observed in a small volume (5 mL) of 50 mM H_2SO_4(aq) electrolyte that contained 56.6 μM of pre-existing nitrate ions after purging with $^{14}N_2$ gas for 20 min. Furthermore, we used a chemiluminescence analyzer to measure the NO(g) and NO_2(g) concentrations in both Ar and $^{14}N_2$ gas cylinders (ultra-high purity, Airgas). The concentrations of NO(g) in both the Ar and $^{14}N_2$ cylinders was measured as 0 ppb, whereas ~ 1.3 and 3.1 ppb of NO_2(g), respectively, were detected. As a reference, the concentrations of NO(g) and NO_2(g) in

the laboratory air were 0 and 4.8 ppb, respectively. The results showed that both $^{14}N_2$(g) and Ar gases were free of NO(g) and contained lower levels of NO_2(g) than the laboratory air.

After 20-min electrochemical experiments with electrodes introduced into electrolyte, increased concentrations of nitrate ions were found in all electrolyte samples. However, we did not find a direct correlation between these increased nitrate concentrations and the ammonium ($^{14}NH_4^+$) yields.

To exclude active nitrate reduction by the CoMo electrode, we performed an additional electrochemical experiment in which a CoMo electrode was held at -0.54 V vs. RHE in 50 mM H_2SO_4(aq) that additionally contained 40.6 μM of pre-existing nitrate ions (volume=20 mL). The electrochemical experiment was performed without any gas purging to avoid the effects of: (1) HNO_3 removal by purging; and (2) introduction of additional nitrate impurities. After electrochemical experiments, the nitrate concentration slightly increased to 41.9 μM after 20 min of testing, while the ammonium concentration increased from negligible amounts to 3.8 μM (measured by IC). These observations exclude substantial nitrate reduction at the CoMo electrode, which would have reduced the nitrate concentration during production of ammonia.

Collectively, these results show that μM-level nitrate ions were present in the electrolyte (although their concentration can vary at different experimental stages). We however conclude that it is unlikely that these nitrate ions led to the ammonia that was consistently observed in our study.

Table S5. Contamination effect of the plastic polypropylene vials (Thermo Scientific C4000-11) for IC analysis found for 6 different samples, showing consistent increases of ammonium concentration over prolonged storage (10 days).

Sample No.	Initial results [µM]	After 10 days [µM]	Increase [µM]
1	0.3	6.4	6.1
2	5.2	10.3	5.1
3	49.8	65.3	15.5
4	0.4	3.4	3.0
5	0.4	3.8	3.4
6	2.4	6.0	3.6

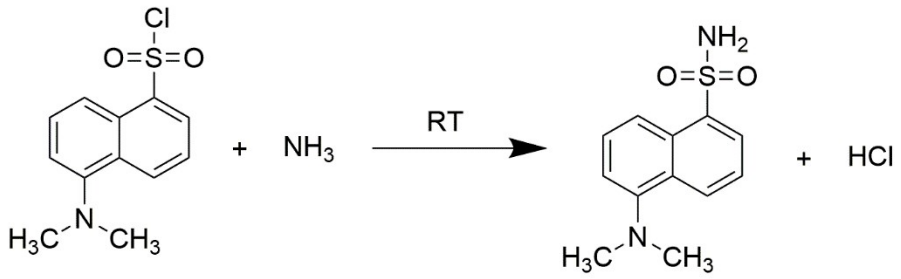

Equation S1. The derivatization reaction of dansyl chloride with ammonia used for UPLC-MS analysis. RT is room temperature.

References

1 G. W. Watt and J. D. Chrisp, *Analytical Chemistry*, 1952, **24**, 2006–2008.

2 W. Yu, N. S. Lewis, H. B. Gray and N. F. Dalleska, *ACS Energy Letters*, 2020, 1532–1536.

3 B. Cao, G. M. Veith, J. C. Neuefeind, R. R. Adzic and P. G. Khalifah, *Journal of the American Chemical Society*, 2013, **135**, 19186–19192.

4 X. Fu, H. Su, W. Yin, Y. Huang and X. Gu, *Catalysis Science & Technology*, 2017, **7**, 1671–1678.

5 S. Podila, S. F. Zaman, H. Driss, Y. A. Alhamed, A. A. Al-Zahrani and L. A. Petrov, *Catalysis Science & Technology*, 2016, **6**, 1496–1506.